

Simulation of Deep Excavation in Sand by Finite Element Using Hardening Soil Model (HSM)

Zuhair Abd Hacheem 

Received on: 23/12 /2010

Accepted on: 6 / 10 /2011

Abstract

Deep excavation is very important problem in geotechnical engineering and use in construction of tunnel and underground structure. This paper study the deep excavation using Plaxis V8.2 engineering program and simulation the soil behavior by Hardening soil model (HSM) that very sensitive to describe the stress path of deep excavation and the model distinguishes between loading and unloading stiffness compares to The Mohr-Coulomb Model (MCM). The parametric study adopt the variation of sand density (loose, medium, and dense), and excavation width ($B = 10, 20, 40, 60, \text{ and } 80 \text{ m}$).

The result conclusions this parameter it's very important on horizontal wall deflection, bending moment of wall, interface stress between soil and wall, heave, and settlement of near ground surface, to make the deep excavation and don't failure and reduce of on horizontal wall deflection, bending moment of wall, heave and settlements of near surface and contort on the near building to attainment the safe design and easy construction with optimum dimensions.

Keywords: Deep excavation, Hardening soil model (HSM), finite elements

تمثيل الحفر العميق في التربة الرملية بطريقة العناصر المحددة باستخدام نموذج تصلب التربة

الخلاصة

يعتبر الحفر العميق من المسائل المهمة في هندسة الجيوتكنك والتي تستخدم لإنشاء الانفاق والمباني تحت الارض في هذا البحث تم دراسة الحفر العميق باستخدام البرنامج الهندسي Plaxis v8.2 بتمثيل التربة بانموذج حديث Hardening Soil Model والذي له قدرة عالية على تمثيل سلوك التربة لمسائل الحفر العميق والتميز بين حالة تسليط الأحمال ورفعها على صلابة التربة مقارنة بانموذج Mohr-Coulomb Model (MCM) الذي لا يميز بين حالات التحميل في هذا البحث تم اعتماد طريقة إسناد الحفر (Braced excavation method) وتثبيت خواص جدران الإسناد والمساند ومراحل الحفر والتي تم اختيارها لتحقيق جميع حالات الدراسة دون حدوث الانهيار فيها لضمان عدم تأثيرها على نتائج البحث مع دراسة تغير الخواص الهندسية للتربة الرملية (كثيف , متوسط , ضعيف) و عرض الحفر ($B = 10, 20, 40, 60, \text{ and } 80 \text{ m}$) وبينت النتائج ان هذه المتغيرات لها تأثيرا كبيرا على كل من الهطول الأفقي و العزوم للجدار و الأجهادات بين التربة والجدار ولهطول قاع الحفر وهطول السطح المجاور للجدار مما يساعدنا على تحقيق الوصول لعمق الحفر المطلوب وعدم حدوث انهيار وتقليل الهطول الأفقي للجدار وتقليل الهطول للجوانب وقاع الحفر والسيطرة على الأضرار للمباني المجاور لتحقيق تصميم امن وسهل التنفيذ من خلال اختار الأبعاد المناسبة.

Introduction

The demand for underground space, for use as transport tunnels, parking garages, storage spaces, etc. in many heavily urbanized areas requires the construction of deep excavation in close proximity to sensitive structures. Advanced excavation techniques, including the use of thick structural diaphragm walls and support construction procedures, are effective methods to reduce deformations in the surrounding soil and damage to adjacent structures. However, in deep excavation and walls embedded in deep soil, the soil movements are difficult to control. The prediction of these movements, in such situations, becomes an important part of design of the support structure as well as the construction monitoring stage. Numerical methods are the only methods available to predict deformations caused by complex construction activities. The usefulness of the mechanical behavior of the soil material and the availability of procedures to model complex construction sequences.

Deep excavation systems

The deep excavation of soil has two main effects. The first is that the removal of the weight of the excavated soil results in a decrease in the vertical stress in the soil beneath the excavation. The second is that the removal of the soil in the excavation results for the soil around the excavation. The purpose of a deep excavation support system is to provide lateral support for the soil around an excavation and to limit movement of the surrounding soil (1). Support systems for deep excavations consist of two main components. The

first is a retaining wall. The second component is the support provided for the retaining wall. Many types of walls are diaphragm (structural slurry), sheet pile, soldier piles and lagging, tangent piles, contiguous piles, and deep soil mixed walls. The principal types of supports are struts (braces), rakers, and tieback anchors (1).

Excavation methods

The following are some commonly used excavation methods

1. Full open cut methods
2. Braced excavation methods
3. Anchored excavation methods
4. Island excavation methods
5. Top - down construction methods
6. Zoned excavation methods

The braced excavation method is the most commonly used among them. Selection of an appropriate excavation method necessarily considers many factors, such as construction budget, allowable construction period, existence of adjacent excavation, availability of construction equipment, area of construction site, conditions of adjacent building, foundation types of adjacent buildings, and so on. Experienced engineers are able to make good selection, based on these factors (2).

Type of support systems

Tie back anchors, ground anchors, struts, props or rakers, berms, basement floors (in top down construction), and soilcrete-slab (jet grouting) are the most common types of support systems. These support systems are schematised in Fig. 1. The relative rigidity of these components and the facings, and their interconnection and packing, is important in determining the amount

of ground movement, and thus the reduction in ground pressure, and the forces and stresses applied to a wall (3).

Duncan and Bentler 1998 (4) indicated that there is a tendency to use struts more frequently than tie back anchors. This is mainly due to the problem associated with the installation of the tie back anchors, i.e., the installation of anchors might lead to settlement or heaving of the ground in built up area. Sometimes it may also be difficult to install tied back anchors in built up areas due to land ownership problem. The use of the top-down construction method has also increased, but still represents a small number. Though the top-down method of construction is widely known in preventing the ground movements effectively, the construction method is relative complicated and there is very limited experience available in practice. (3)

Behavior of excavations

In soil mechanics the two common limits occur due to:

- § Shear failure of the soil, leading to excessive distortion of a structure or a disruption of highways and services;
- § Excessive settlement of the soil, inducing unacceptably high stresses in a structure as a result of differential movement.

For retaining structures, failure is a performance problem, related to either strength or deformation. A retaining structure can fail to perform in a satisfactory way for a number of reasons, associated with the failure of the structure itself, failure of the soil or because of unacceptable deformation. Some possible failure situations in retaining structures are shown in Figure 2. In general, the design of a retaining structure should

considered the following points: moment equilibrium of the system (overturn), horizontal force equilibrium (sliding), vertical equilibrium (bearing capacity), overstress of any part of the structure (bending or shear), and the general stability of the soil around the structure (slope failure, overall stability, basal stability). The stability of the structure should be satisfactory both in short-term and in the long-term. Because many retaining structures are associated with decreased level of total stress, it is normal to carry out long-term analysis in terms of effective stresses and effective strength parameters. This will normally give the worst conditions (Clayton et al. 1993) (5).

On the other hand, a retaining structure may perform unsatisfactorily because of the excessive displacement it undergoes. It is seldom possible to predict such movements of the retained ground with any degree of confidence analytically. To reduce the excessive displacement, it is common to apply a large factor of safety against failure to the critical area. For example a total factor of safety of 1.5 to 2.0 is applied on the passive resistance to reduce tilt and lateral displacement of the wall in sands and stiff clays. The design of a retaining wall include the selection of the type of the retaining wall, determination of the depth of penetration of the wall, determination of the section size of the wall, determination of the strut or anchor load, prediction of the deflection of the wall and ground movements, and checking the stability of the excavation. In the following subsequent sections, the most important components of retaining structures design, namely (3)

- a) Earth pressure, strut and anchor load, and bending moment of the wall.
- b) Ground movements in and around an excavation.
- c) Stability of retaining structures, in particular basal stability, and
- d) Safety factor in the design of retaining structures are presented.

The constitutive soil models used in PLAXIS program

The finite element code PLAXIS professional version is used for back analysis the practical projects and for performing parametric studies in this paper. The PLAXIS program contains constitutive soil models from simple linear elasticity to advanced elasto-plastic cap soil models. The details of each soil model can be found in PLAXIS users manual (Vermeer and Brinkgreve 1995 (6); Brinkgreve and Vermeer 1998 (7); Brinkgreve 2002 (8)). A summary of the basic features, the failure criteria, the required soil parameters, range of application, etc. of the three main soil models available in PLAXIS are given in Table 1. In the earlier version of PLAXIS, up to version 6.0, the hard soil model (HSM) and the soft soil model (SSM) are primarily used for hard soils such as gravels, sands and heavily overconsolidated cohesive soils, and for normally consolidated and lightly overconsolidated clays respectively. This is mainly because the HSM was developed on the assumption that plastic straining is dominated by shearing and associated volumetric strains are relatively small and cause dilation rather than compaction which is a property of non-cohesive and heavily consolidated cohesive soils. On the other hand the SSM was developed based on the assumption of compression hardening, which is mainly a property of soft clays. In

contrast to this basic formulation of the models, (Freiseder (1998) (9)) believed that the HSM give more realistic results on deformation of the wall and settlement of ground behind the wall in an excavation in normally consolidated clay than the other models. In the PLAXIS version 7 and above, the SSM was superseded by the HSM, and the HSM comes out as advanced double hardening model applied for all types of soils, i.e., it is now based on shear as well as compression hardening, a property of both hard soils and soft soils. In these versions, the name hard soil model is replaced by the hardening soil model. The HSM assumes a uniform expansion of the yield surface in all direction, i.e., it is based on isotropic hardening. The soft soil model is also modified to include time dependent behavior of soft soils and it is called the soft soil creep model (SSCM). The Mohr-Coulomb model (MCM), which is an elastic- perfect plastic model, can be applied for all types of soils (3).

Freiseder 1998 had compared the three soil models (HSM, SSM and MCM, see Table 1) available in PLAXIS using an idealized excavation in normally consolidated lacustrine clay which is supported by diaphragm wall. He concluded that the HSM provides a realistic result as far as the horizontal deflection of the wall and settlement of the surface behind the wall are concerned, though it was first developed to model the behavior of non-cohesive soils and overconsolidated clays. He further commented that the response of the HSM to stress path at some points with in the excavation is more realistic than the other models (3).

Hardening soil model (HSM)

Constitutive equation which model accurately the behavior of soils are essential if reliable numerical predictions of performance are to be achieved for practical geotechnical problems. Significant difficulties in developing such models are associated with the complexity of soil behavior observed from both laboratory tests and field observations (Youssef M.A. Hashash (1992)) (10).

The hardening soil model is an advanced model for simulating the behavior of different type of soil, both soft soils and stiff soils, (Schanz 1998) (11). When subjected to primary deviatoric loading soil shows a decreasing stiffness and simultaneously irreversible plastic strains develop. In the special case of drained triaxial test the observed relationship between the axial strain and deviatoric stress can be well approximated by a hyperbola. Such a relationship was first formulated by (Kondner 1963) (12) and later used in the well known hyperbolic model (Duncan and Chang 1970) (13). the hardening soil model, however, supersedes the hyperbolic model by far. Firstly by using the theory of plasticity rather than theory of elasticity. Secondly by including soil dilatancy and thirdly by introducing a yield cap (14).

In contrast to the Mohr-Coulomb model, the hardening soil model also accounts for stress dependency of stiffness module. This mean that all stiffnesses increase with pressure. Hence, all input stiffnesses relate to a reference stress, being usually taken as 100 kPa (1 bar).

The parameters of the Hardening Soil Model :

Failure parameters are as in Mohr-Coulomb Model

- C : Effective cohesion
- Φ : Effective angle of internal friction
- Ψ : Angle of dilatancy

Basic parameter for soil stiffness

- E_{50}^{ref} : Secant stiffness in standard drained triaxial test
- E_{ode}^{ref} : Tangent stiffness for primary oedometer loading
- m : Power for stress level dependency of stiffness

Advanced parameter

- E_{ur}^{ref} : Unloading / reloading stiffness (default $E_{ur}^{ref} = 3 E_{50}^{ref}$)
- n_{ur} : Poisson's ratio for unloading – reloading (default $n_{ur} = 0.2$)
- P^{ref} : Reference stress for stiffnesses (default $P^{ref} = 100$ stress units)
- K_o^{nc} : K_o Value for normal consolidation (default $K_o^{nc} = 1 - \sin j$)
- R_f : Failure ratio q_f / q_a (default $R_f = 0.9$)
- $S_{tension}$: Tensile strength (default $S_{tension} = 0$ stress units)
- $C_{increment}$: As in Mohr-Coulomb model (default $C_{increment} = 0$)

$$E_{50} = E_{50}^{ref} \left[\frac{C \cdot \cos j - s'_3 \cdot \sin j}{C \cdot \cos j + P^{ref} \cdot \sin j} \right]^m$$

$$E_{ur} = E_{ur}^{ref} \left[\frac{C \cdot \cos j - s'_3 \cdot \sin j}{C \cdot \cos j + P^{ref} \cdot \sin j} \right]^m$$

$$E_{oed} = E_{oed}^{ref} \left[\frac{C \cdot \cos j - s'_3 \cdot \sin j}{C \cdot \cos j + P^{ref} \cdot \sin j} \right]^m$$

In the excavation problem the deformation mesh by hardening soil model shows that there is limited heave at the bottom of the excavation. Most of the deformation is caused by the horizontal moment of the diaphragm wall, which pushes the soil up. The vertical heave at the bottom further away from the wall is very low as compared to the results in the Moher-Coulomb model (14).

The difference can be explained by the fact that, in contrast to the Moher-Coulomb model, the Hardening Soil Model distinguishes between **loading and unloading stiffness** (14)

Constitutive relations for interface elements

Clough and Duncan 1971 (15) studied the interaction between the wall and the backfill material with the help of shear box test and showed that the stress-displacement behavior of the interface is similar to the stress-strain behavior of soils. In order to implement the interface behavior in the finite element analysis of retaining walls, Clough and Duncan 1971 (15) developed a non-linear, stress dependent stiffness, hyperbolic stress-strain constitutive relation to represent interface behavior similar to those developed by Duncan and Chang 1970 (13) to model the stress-strain behavior of soils. Like the behavior of soils, interface behavior may also be represented by complex advanced models. However, Gens et al. 1989 (16) underlined the use of less complex models. They used an elastic-

perfectly plastic model with out dilatancy effect in their finite element study of the soil-reinforcement interaction. In PLAXIS the MCM is used to represent the interface behavior, whatever model is applied to represent the soil behavior (3).

Case studies

Using (PLAXIS) geotechnical engineering programs to investigate the influence of the size of the excavation width (B) and the sand state on the deformation behavior of an excavation, an idealised excavation shown in Fig.3 has been chosen. The ground is assumed a homogeneous sand soil with the groundwater table located at 1.0 m below the ground surface. The excavation 20 m deep is supported by a diaphragm wall 0.8 m thickness with a total length of 30 m, with an embedment depth of 10 m and with two level of struts. A drained type of analysis has been used, because it is believed that this condition is most unfavorable condition for excavations. The reference sand soil parameters are adopted from Table 2 for the HSM (14). The stiffness of the soil were taken as it is for the interface element, whereas the shear parameter were reduced by a factor of 1/3 in the MCM. The diaphragm wall and the struts are assumed to behave linear-elastic with the material properties in Table 3 and 4.

Three type of sand soil (Loose, Medium, and Dense) and five excavation width B = 10, 20, 40, 60, and 80 m has been considered in the parametric study. For each case (15 cases) of the excavation width, the sand soil state and boundary condition are varied according to the fig.3. Details of the construction sequence are listed in Table 5.

Results and Discussion Wall bending moment

In the analysis in this study carried out, one of the main constraints associated with the solution proposed consists in the fact that it is not possible to modify structurally the diaphragm wall that has been already case in place. The evaluation of the bending moment acting on the wall represent therefore one of the main elements that need to be considered. Figures (4 - 8) plots the bending moment acting on the wall in last stage of excavation. The bending moment is defined as positive when the tension face of the wall is on the excavation side.

Lateral wall deflection

Figures (9 - 13) summarizes the wall deflected profiles for 15 different cases.

Settlement and heave

Figures (14 - 18) show the settlement of the ground surface behind the wall, figures (19 - 23) show the heave at the bottom of excavation.

Interfaces surface

Another important factor affecting the performance of deep excavation are in the interfaces Figures (24 - 33) describes the effective normal stresses and shear stresses for the parametric study, where the effective normal stresses are the effective normal stresses perpendicular to the interface and the shear stresses are the shear stresses in the interfaces.

Conclusions

The parametric study presented in this treatise numerically assessed the efficiency of the variation of excavation width ($B = 10, 20, 40, 60,$ and 80 m) with variation of sand density (Loose, Medium, Dense) on the wall, interfaces, heave, and settlement using hardening soil model

(HSM). The main results of the numerical study were as follow

1. Wall structure
 - a) The horizontal deflection of wall increases about 52 % with increase of the width (between 10 and 80 m) of excavation and decrease about 45 % with increase in the sand density (between Loose and Dense).
 - b) The bending moment increases about 9 % with increase of the excavation width (between 10 and 80 m), and decrease about 30 % with increase in the sand density (between Loose and Dense).
2. Interfaces surface
 - a) The shear stresses in the interfaces surface between soil and wall is not influenced by the variation of excavation width and increase about 60 % with increase in the sand density (between Loose and Dense).
 - b) The normal stress in the interfaces surface between soil and wall is not influenced by the variation of excavation width and increase about 20 % with increase in sand density (between Loose and Dense).
3. Heave and Settlement
 - a) Heave at the excavation bottom increases about 42 % with increase of the excavation width (between 10 and 80 m) and decreases about 41 % with increase in the sand density (between Loose and Dense).
 - b) The settlement at the surface tends to increases about 65 % with increasing in excavation width (between 10 and 80 m) and decrease about 50 % with increase in sand density (between Loose and Dense).

References

- [1]David J. Bentler (1998) "Finite element analysis of deep excavation" Ph.D. thesis Virginia polytechnic institute and state university.
- [2]Chaug-Yu Ou (2006) "Deep excavation theory and practice" book, Taylor and Francis Group, London, UK.
- [3]Hans-Georg Kempfert and Berhane Gebreselassie (2006) "Excavation and foundation in soft soil" book, Springer-Verlag Berlin Heidelberg 2006 Printed in The Netherlands.
- [4]Duncan JM, Bentler DJ (1998) "Evolution of deep excavation technology". International Conference on Soil-Structure Interaction in Urban Civil Engineering, Darmstadt Geotechnics, Darmstadt, pp 139 – 150.
- [5]Clayton CRI, Milititsky J, Woods RI (1993) "Earth pressure and earth retaining structures".2nd edn., Chapman & Hall, London.
- [6]Vermeer PA, Brinkgreve RBJ (1995) Hand book of "the finite element code for soil and rock analysis" "PLAXIS" Balkema Publisher.
- [7]Brinkgreve RBJ, Vermeer PA (1998) Hand book of the finite element code for soil and rock analysis "PLAXIS", Balkema, Rotterdam.
- [8]Brinkgreve RBJ (2002) Hand book of the finite element code for soil and rock analysis "PLAXIS" Balkema, Rotterdam.
- [9]Freiseder MG (1998) Ein Beitrag zur numerischen Berechnungen von tiefen Baugruben in weichen Bden. Gruppe Geotechnik Graz, Institute für Bodenmechanik und Grundbau, Heft 3
- [10]Youssef M.A. Hashash (1992) "Analysis of deep excavation in clay" Ph.D. thesis at Massachusetts Institute of Technology.
- [11]Schanz, T., Vermeer, P.A., (1998) "Special issue on Pre-failure deformation behaviour of geo materials" Geotechnique 48, pp. 383-387.
- [12]Kondner RL, Zelasko JS (1963) "A hyperbolic stress-strain formulation for sands". Proc. 2nd Pan-American Conference on Soil Mechanics and Foundations Engineering, Brazil, Vol. I, pp 289 – 324.
- [13]Duncan JM, Chang CY (1970) "Non-linear analysis of stress and strain in soils". Journal of the Soil Mechanics and Foundation Division, ASCE 96-SM5, pp 1629 – 1653.
- [14]PLAXIS (2006) Version 8.2 Professional version (www.Plaxis.nl), PLAXIS full manual.]
- [15]Clough GW, Duncan JM (1971) "Finite element analysis of retaining wall behaviour". Journal of Soil Mechanics and Foundation Engineering, ASCE 97-SM12, pp 657 – 673.
- [16]Gens A, Carol I, Alonso EE (1989) "An interface element formulation for the analysis of soil-reinforcement interaction". Computers and Geotechnics. Elsevier Science Publishers Ltd, England, pp 133 – 151.

Table 1. Summary of the main constitutive soil models in PLAXIS program (3)

	Hardening soil model (HSM)	Soft soil creep model	Moher Coulomb model (MCM)
Type of model	<ul style="list-style-type: none"> Elasto-plastic strain hardening cap model 	<ul style="list-style-type: none"> Elasto-plastic work hardening cap model 	<ul style="list-style-type: none"> Elastic perfect plastic
Basic features	<ul style="list-style-type: none"> Stress dependent stiffness according to power law $E = E^{ref} \left[\frac{c' \cdot \cos j - s}{c' \cdot \cos j + p} \right]$ <ul style="list-style-type: none"> Plastic straining due to primary deviatoric loading Plastic straining due to primary compression Elastic unloading / reloading Hyperbolic stress-strain relation and soil dilatancy 	<ul style="list-style-type: none"> Stress dependent stiffness (logarithmic compression behaviour) Distinction between primary loading and unloading / reloading Secondary (time-dependant) compression Memory of pre-consolidation. 	<ul style="list-style-type: none"> Offers a special option for the input of a stiffness increasing with depth. Soil dilatancy.
Failure criterion	<ul style="list-style-type: none"> Moher-Coulomb 	<ul style="list-style-type: none"> Moher-Coulomb 	<ul style="list-style-type: none"> Moher-Coulomb
Cap yield surface	$F_c = \frac{\bar{q}^2}{a^2} + p^2 - p_p^2 ;$ $\bar{q} = s_1 + (d-1) \cdot s_2 - d \cdot s_3 ;$ $d = \frac{3 + \sin j}{3 - \sin j}$ <ul style="list-style-type: none"> a is a model parameter that relates to K_o p_p is isotropic pre-consolidation stress P is the effective mean stress 	$F_c = \frac{q^2}{M^2 \cdot (p + C \cdot \cot j)} + p - p_p$ <ul style="list-style-type: none"> M is a model parameter that relates to K_o p_p is isotropic pre-consolidation stress P is the effective mean normal stress q is shear stress 	<ul style="list-style-type: none"> None
Flow rule	<ul style="list-style-type: none"> Non-associated in shear hardening associated in compression hardening (cap) 	<ul style="list-style-type: none"> associated 	<ul style="list-style-type: none"> Non-associated
State of stress	<ul style="list-style-type: none"> Isotropic 	<ul style="list-style-type: none"> Isotropic 	<ul style="list-style-type: none"> Isotropic
hardening	<ul style="list-style-type: none"> Isotropic ; shear and compaction 	<ul style="list-style-type: none"> Isotropic ; compaction 	<ul style="list-style-type: none"> None
Soil parameters	<ul style="list-style-type: none"> $c', j', \gamma, E_{50}^{ref}, E_{ur}^{ref}, E_{oed}^{ref}, m, \lambda$ 	<ul style="list-style-type: none"> $c', j', \gamma, l^*, k^*, m^*, v_{ur}, M, K_o$ 	<ul style="list-style-type: none"> c', j', γ, E, ν
Rang of application	<ul style="list-style-type: none"> All type of soils 	<ul style="list-style-type: none"> Normally consolidated or lightly overconsolidated clayey soils 	<ul style="list-style-type: none"> All type of soils

Table (2) Hardening soil parameter for sands of different densities (14)

<i>Parameter</i>	<i>Loose</i>	<i>Medium</i>	<i>Dense</i>	<i>Unit</i>
E_{50}^{ref} (for $P_{ref} = 100$ kPa)	20000	30000	40000	kN/m ²
E_{ur}^{ref} (for $P_{ref} = 100$ kPa)	60000	90000	120000	kN/m ²
E_{oed}^{ref} (for $P_{ref} = 100$ kPa)	20000	30000	40000	kN/m ²
Cohesion C	0.0	0.0	0.0	o
Friction angle Φ	30	35	40	o
Dilatance angle Ψ	0	5	10	-
Poisson's ratio ν_{ur}	0.2	0.2	0.2	-
Power m	0.5	0.5	0.5	-
K_o^{nc} (using Cap)	0.5	0.43	0.36	-
Tensile strength	0.0	0.0	0.0	kN/m ²
Failure ratio	0.9	0.9	0.9	-

Table (3) Material properties of the diaphragm wall adopt in the research

<i>Parameter</i>	<i>Name</i>	<i>Value</i>	<i>Unit</i>
Type of behavior	<i>Material type</i>	Elastic	
Normal stiffness	EA	7.5×10^6	kN/m ²
Flexural rigidity	EI	1×10^6	kNm ² /m
Equivalent thickness	d	1.265	m
Weight	w	10.0	kNm/m
Poisson's ratio ν_{ur}	ν	0.0	-

Table (4) Material properties of the strut adopt in the research

<i>Parameter</i>	<i>Name</i>	<i>Value</i>	<i>Unit</i>
Type of behaviour	<i>Material type</i>	Elastic	
Normal stiffness	EA	3.801×10^6	kN
Flexural rigidity	L_s	2.0	m
Maximum force	$F_{max,comp}$	1×10^6	kN
	$F_{max,tens}$	1×10^6	kN

Table 5 Construction Sequence adopt in the research.

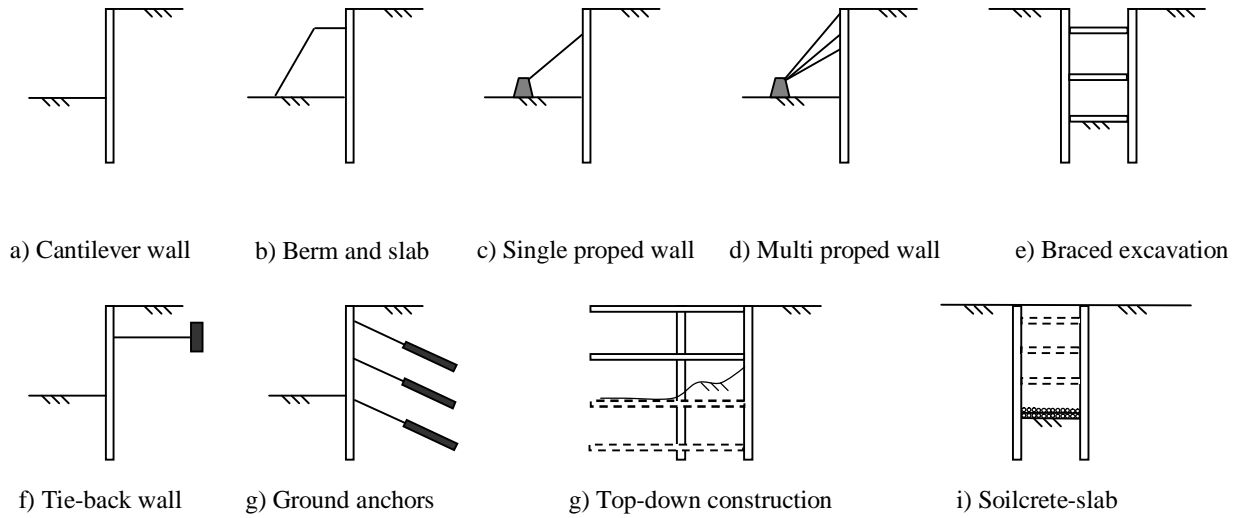


Figure (1) Common types of wall support schemes

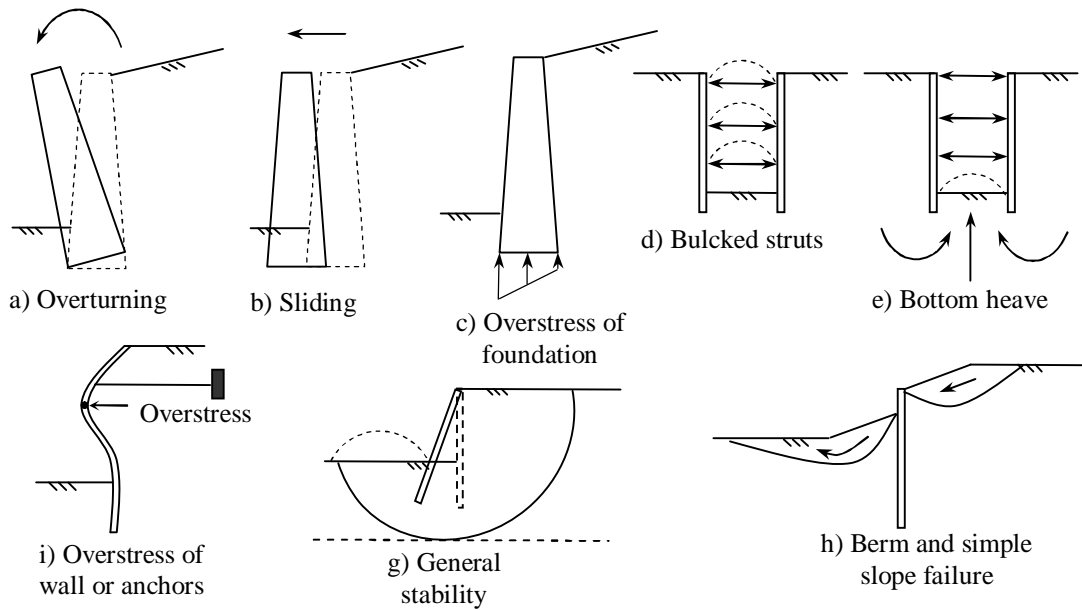


Figure (2) Common types of Failures in supported excavations

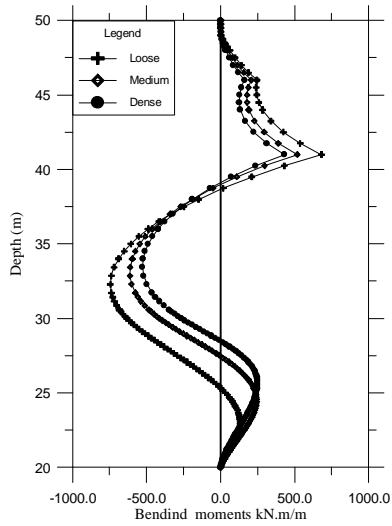


Figure (4) Bending moments for B = 10 m

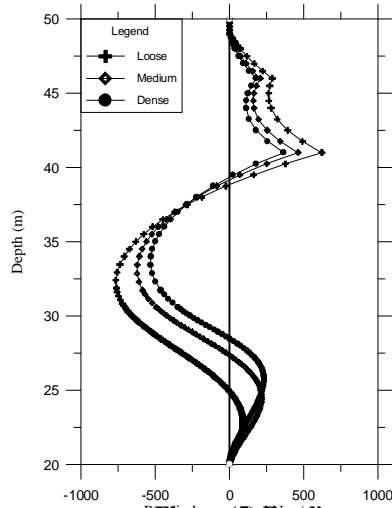


Figure (5) Bending moments for B = 20 m

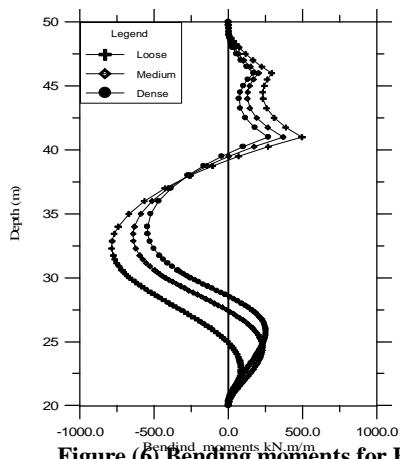


Figure (6) Bending moments for B = 40 m

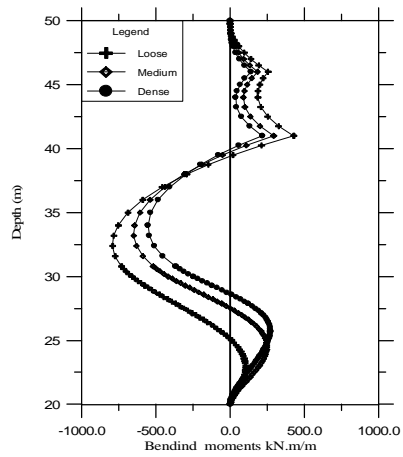
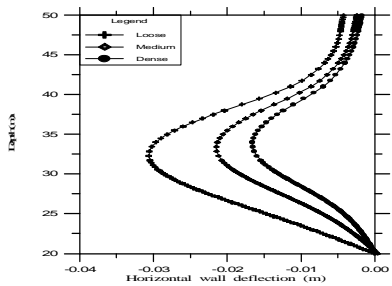


Figure (7) Bending moments for B = 60 m



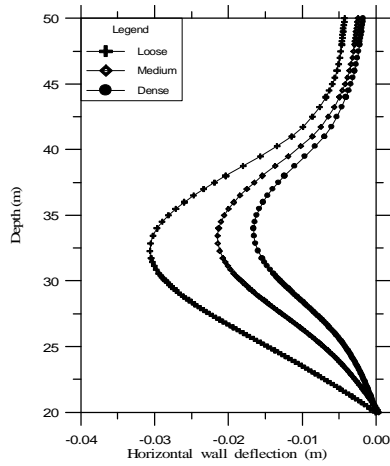


Figure (8) Bending moments for B = 80 m

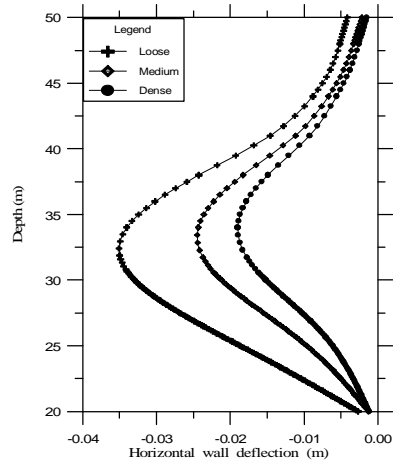


Fig (9) Horizontal wall deflection for B = 10 m

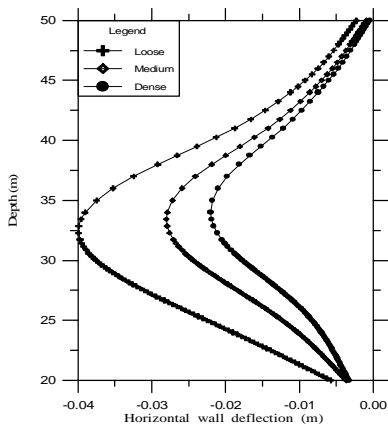


Fig (10) Horizontal wall deflection for B = 20 m

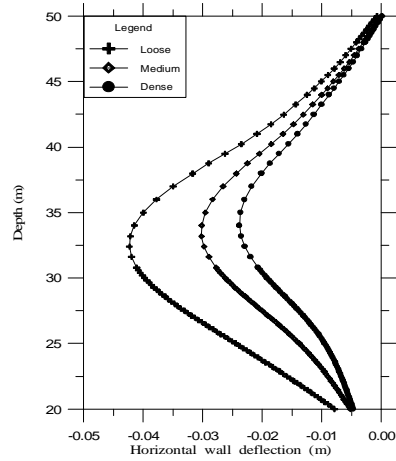


Fig (12) Horizontal wall deflection for B = 60 m

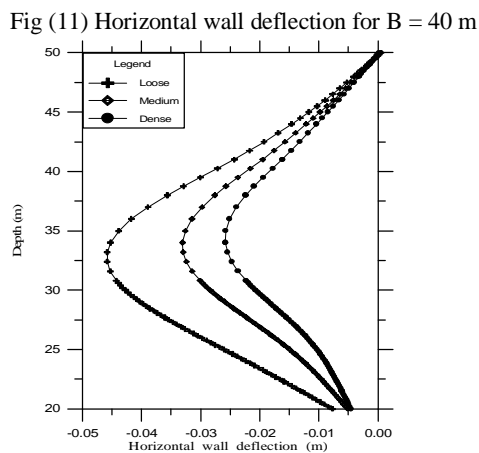


Fig (13) Horizontal wall deflection for B = 80 m

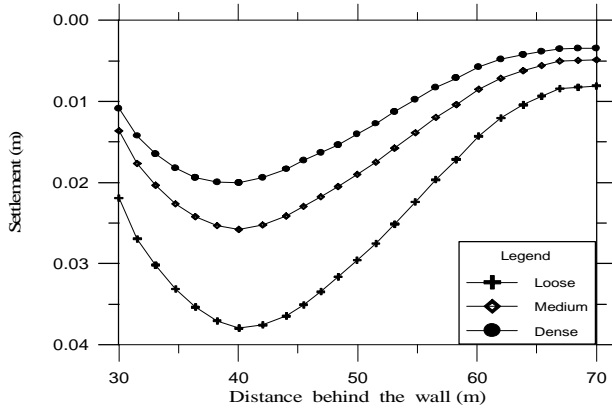


Figure (15) Settlement of surface B =20 m

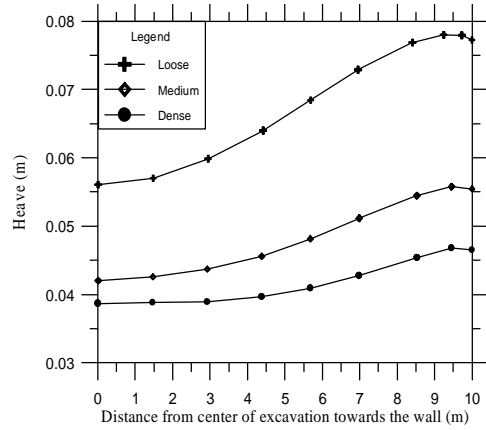


Figure (16) Settlement of surface B =40 m

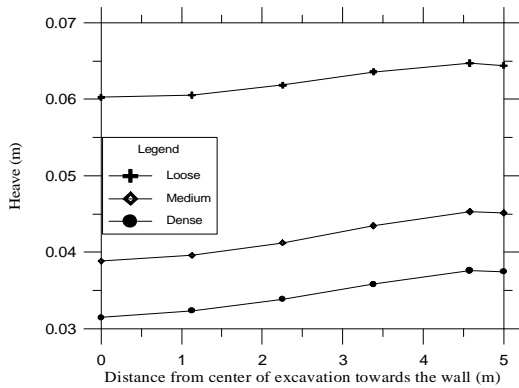


Figure (17) Settlement of surface B

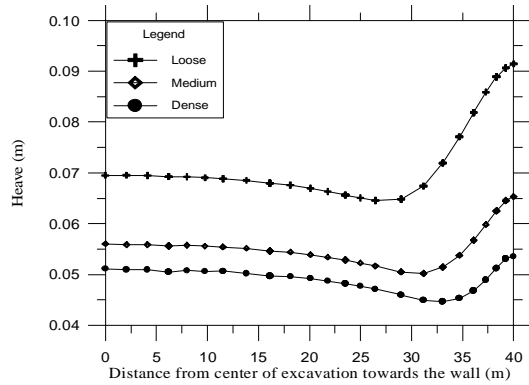


Figure (18) Settlement of surface B =80 m

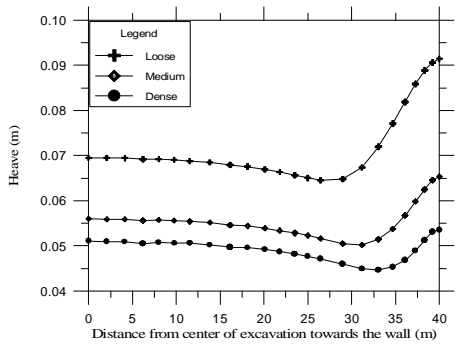


Figure (19) Heave for B = 10 m

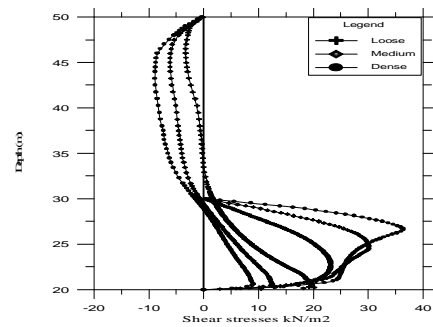


Figure (20) Heave for B = 20 m

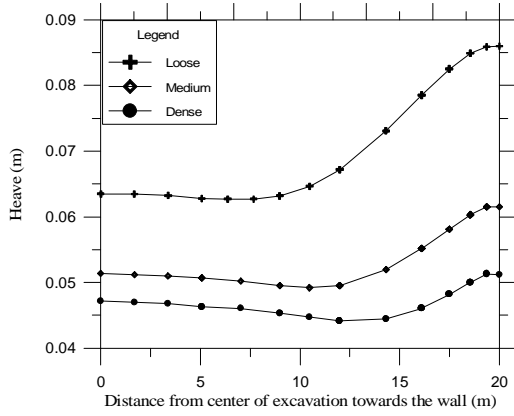


Figure (21) Heave for B = 40 m

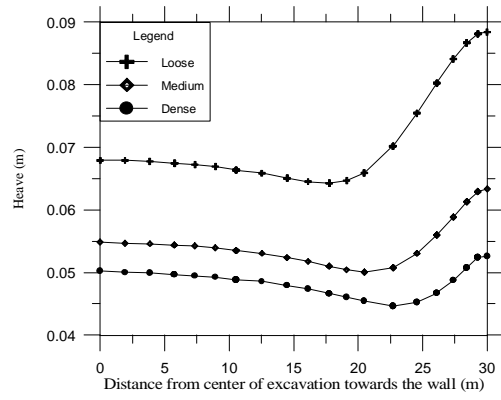


Figure (22) Heave for B = 60 m

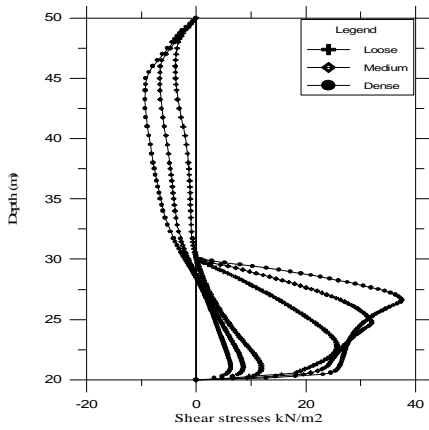
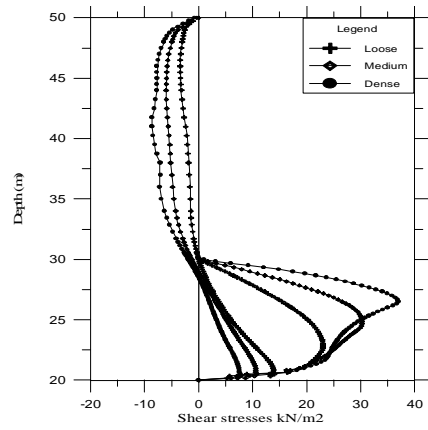


Figure (23) Shear stresses for B=80



Figure(24) Shear stresses for B=10

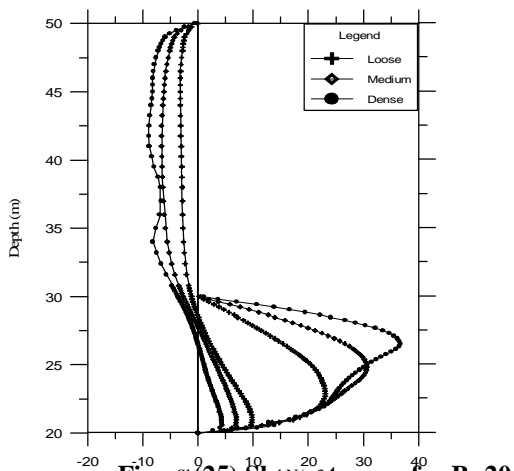


Figure (25) Shear stresses for B=20

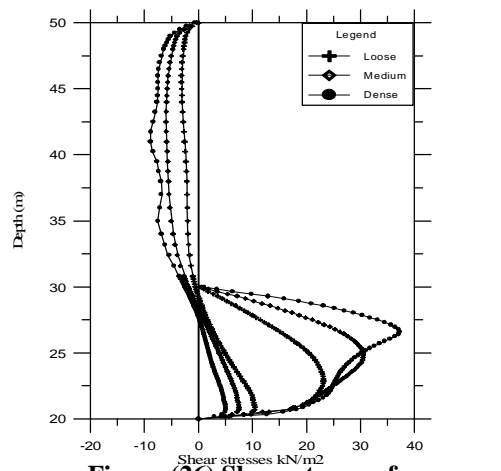


Figure (26) Shear stresses for B=40

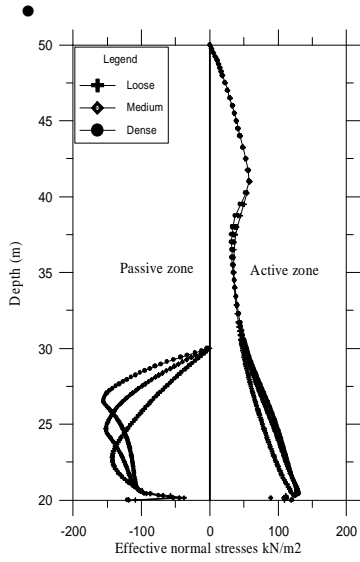


Figure (27) Shear stresses for

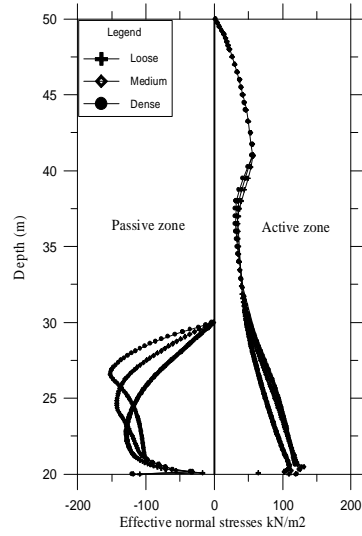


Figure (28) Shear stresses for

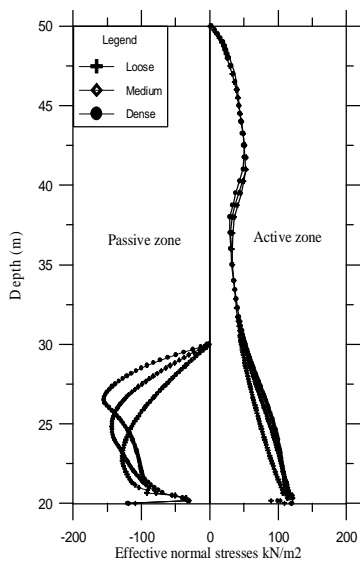


Figure (29) Effective normal stresses for B=10 m

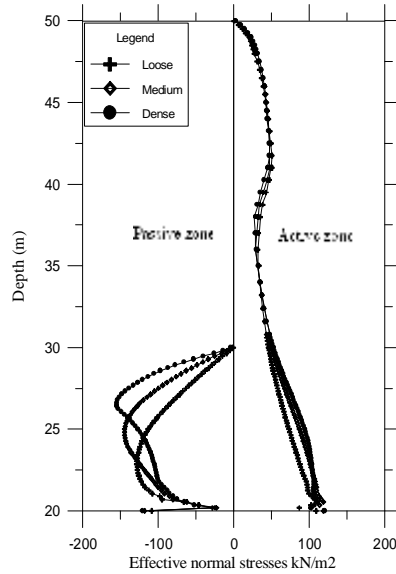


Figure (30) Effective normal stresses for B=20 m

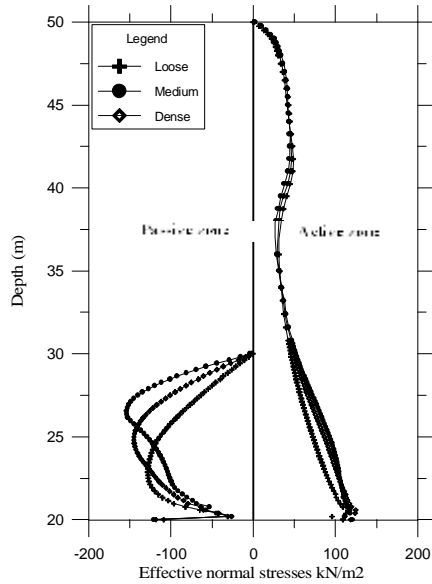


Figure (31) Effective normal stresses for B=40 m

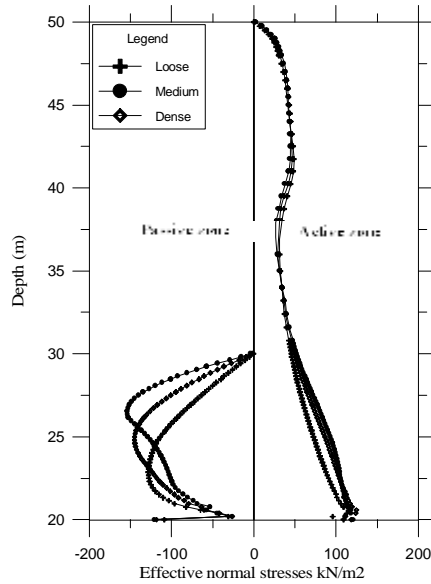


Figure (32) Effective normal stresses for B=60 m

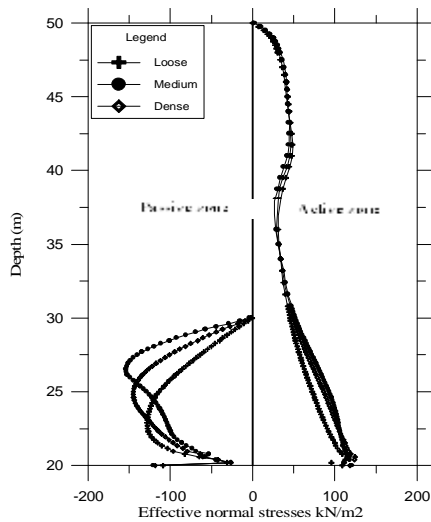


Figure (33) Effective normal stresses for B=80 m